JET–R(00)01

J G Cordey
T C Hender
D C McDonald

Validation of 1999 JET Gas Box Divertor Data

JET–R(00)01

Validation of 1999 JET Gas Box Divertor Data

Compiled by

J G Cordey, T C Hender, D C McDonald.

Staff involved in data validation:

S. J. Allfrey, B. Alper, Y. Baranov, A. Bickley, C. Challis, M. Charlet, J.P.Coad, I. Cof fey, J. Conboy, S.R. Cooper, V. Drozdov, J.Fessey , W.Fundamenski, R.D. Gill, A. Gondhalekar, C.W.Gowers, K. Guenther, N. Hawkes, O.N. Jarvis, M.F.Johnson, T.T.C. Jones, K.D. Lawson, G. Lloyd, P.J. Lomas, J. Mailloux, G. Matthews, A.Meigs, P. Morgan, G.F. Neill, M.O'Mullane, R. Prentice, M.F.Stamp, D. Stork, P . Stubberfield, D. Summers, P.R. Thomas, K-D Zastrow

EURATOM/UKAEA Fusion Association,
Culham Science Centre, Abingdon, Oxon. OX14 3DB

May 2000

PREFACE

As part of the winding-up of the JET Joint Undertaking, an agreement was established with UKAEA to validate the 1999 Gas Box data and make a descriptive analysis of the data. This report constitutes one of the deliverables specified under the agreement and describes the work undertaken on validating the data.

1. INTRODUCTION

Over many years the JET Joint Undertaking established procedures for checking and validating its experimental data. These have been largely followed by UKAEA in validating the 1999 Gas Box data. The validation process is overseen by a Data Co-ordination Committee - this group has met twice during 2000 with a further meeting scheduled for May 2000. A sub-group has also been formed to consider a long standing problem relating to why the centroid of neutron emission does not coincide with the magnetic axis predicted by the EFIT equilibrium reconstruction code (see Section 2.5).

The data validation process essentially divides into:-

- Global checks of overall data consistency, for example by comparing the same quantity measured by 2 different diagnostics and looking for long term trends in the ratios of these quantities and in individual quantities such as Z_{eff}.
- Checks by the Responsible Officers for each diagnostic of the calibration of that diagnostic etc

Checks of global data quality are reported in the next section, then in section 3 individual reports are made for each data item, and finally in section 4 a summary is given. Throughout, the level data consistency achieved by the Joint Undertaking is used as measure of the quality of the 1999 data.

2. GLOBAL DATA QUALITY CHECKS

A valuable method for finding systematic inconsistencies in the data is to compare the same quantity measured by 2 different methods; such checks comparing different methods for measuring plasma energy content, electron temperature and density are reported here. Also long term trends in quantities can indicate a change of diagnostic calibration; a key check of this type is on Z_{eff} and that is reported in this section. Finally, TRANSP calculations give an overall indication of data consistency and some comparisons are reported here.

2.1 Magnetics Data Quality

A good test of the quality of the magnetics data is the comparison of the predicted plasma energy from EFIT with the direct diamagnetic loop measurement. Comparison with previous year's data shows no degradation in the quality of agreement between 1997, 98 or 99 (Fig 2.1)

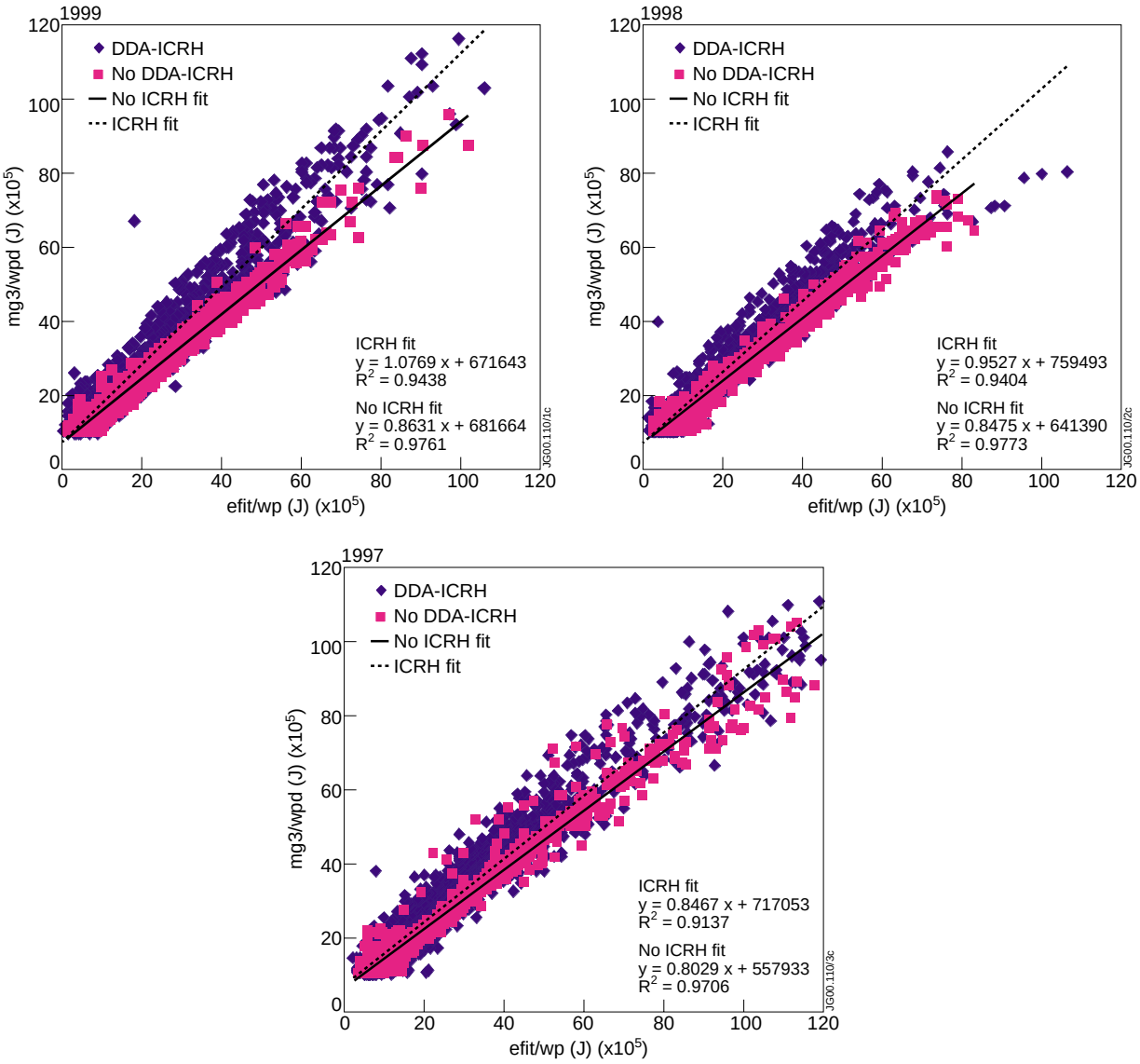

Fig 2.1 Comparison of plasma stored energy from the diamagnetic loop (MG3/WPD) with the EFIT prediction (EFIT/WP). The pink squares are non-ICRH pulses while the blue diamonds have ICRH applied

It can be seen that there is no reduction in the quality of the EFIT fits between 1999 and previous years. It can also be seen that the agreement is much better if ICRH pulses are excluded in the comparison. This can be understood in terms of pressure anisotropy - without ICRH the pressure is close to isotropic (essentially by chance the JET beam ions are have $P_{\perp} \sim 2P_{||}$), while with the ICRH it can be strongly anisotropic (particularly in Optimised Shear discharges - the most common use for ICRH heating). The definition of the EFIT magnetic energy (W_{MHD}) and that measured directly from the diamagnetic loop (W_{DIA}) are:-

$$W_{MHD} = \frac{3}{4} W_{\perp} + \frac{3}{2} W_{||}$$

$$W_{DIA} = \frac{3}{2} W_{\perp}$$

In the isotropic limit these are equal but with ICRH where ($W_{||}$~0) then W_{DIA}>W_{MHD} as found in Fig 2.1. There is an important point here that the *diamagnetic loop signal (MG3/WPD) should not be used to determine stored energy*, β etc when strong anisotropy is expected, instead:

$$W = \frac{2}{3} W_{MHD} + \frac{1}{3} W_{dia}$$

should be used.

2.2 Temperature Data

The quality of the temperature data can be assessed by comparing the ECE temperature data with LIDAR data (Fig 2.2 and 2.3)

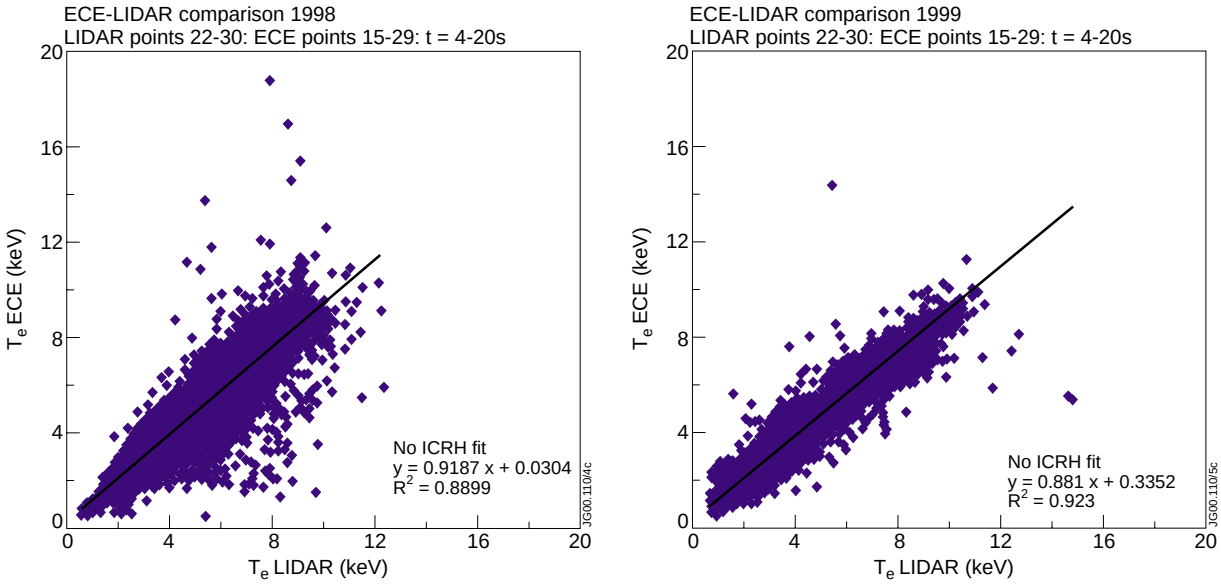

Fig 2.2 Comparison of ECE and LIDAR temperature data from 1998 and 1999, for all shots in CPF.

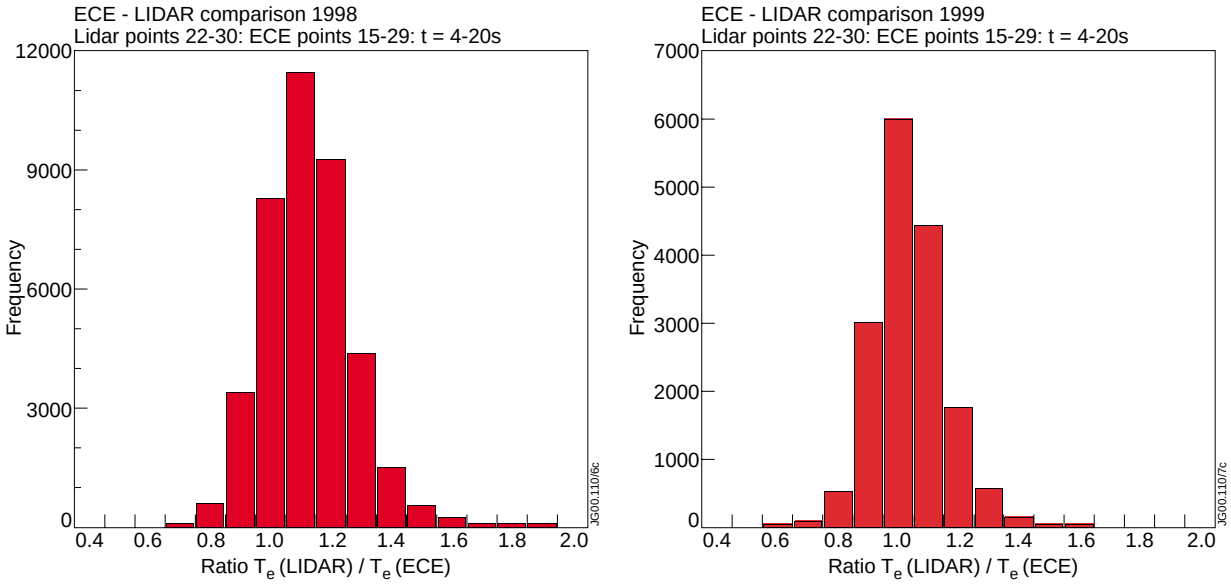

Fig 2.3 Bar chart form of the previous figure (2.2) to show better the large number of measurements that agree.

It can be seen that overall the data quality has improved in 1999.

2.3 Density Data

Similarly the quality of the density data can be checked by comparing the LIDAR and interferometer measurements (Fig 2.4)

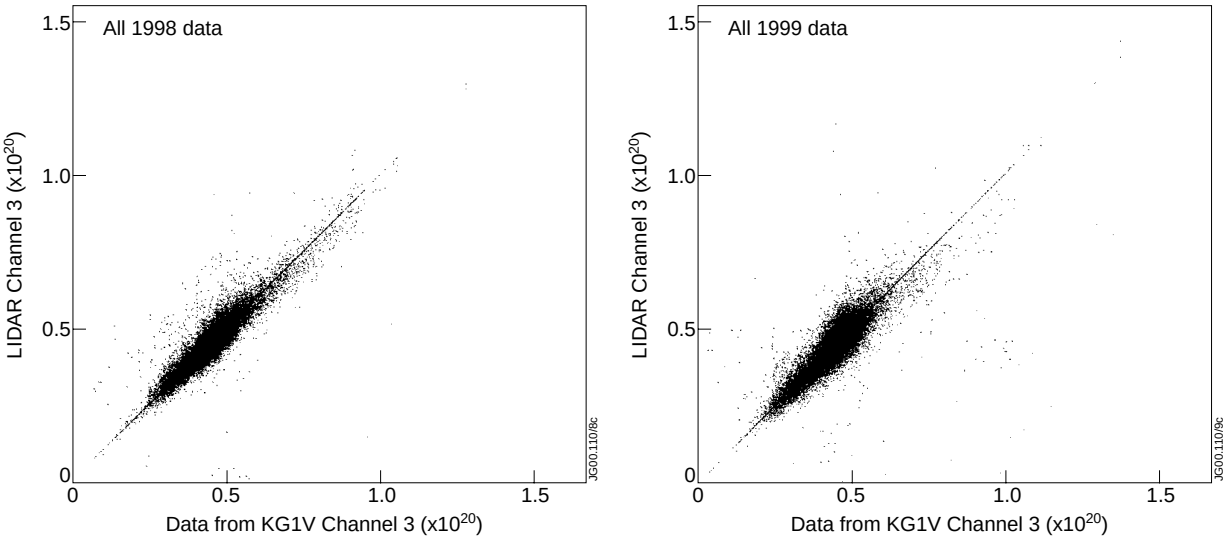

Fig 2.4 Comparison of LIDAR and interferometer density measurements at R=3.02m, for t=2-20s for all shots in the CPF in the indicated years.

It can be seen that there is no significant difference in the scatter of data between 1998 and 1999. The density data quality can also be checked by looking the ratio of the LIDAR and interferometer measurements as a function of time (Fig 2.5).

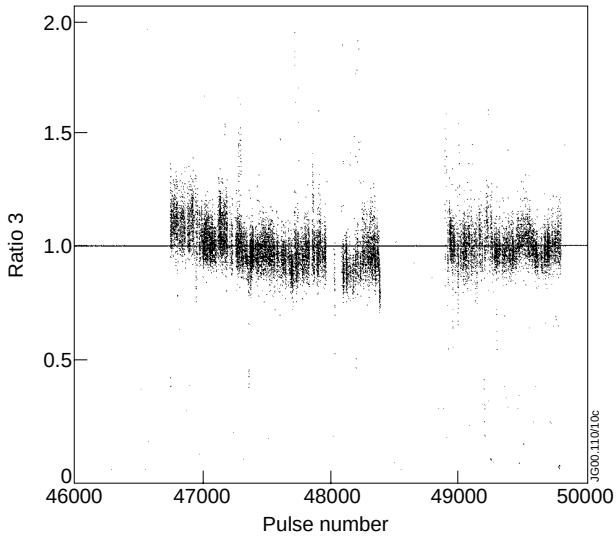

Fig 2.5 Ratio of LIDAR to interferometer data at R=3.02m. A slight drift of the data (within accepted error bars) is evident from about pulse 47,000 to 48,000. A recalibration corrected this drift from about pulse 49,000

2.4 Z_{eff}

A comparison of horizontal and vertical Bremstrahlung measurements shows no systematic drifts in time (Fig 2.6), indicating window transmission corrections are correct.

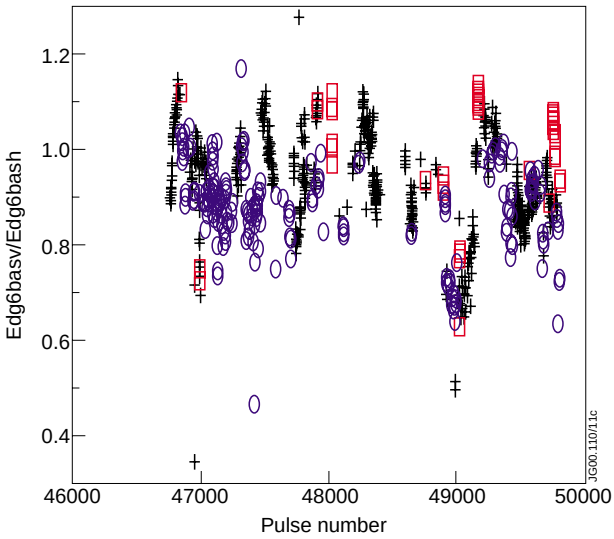

Fig 2.6 Comparison of Bremstrahlung measurements on vertical and horizontal chords in the limiter phase at t=7-8s. The symbols are ❍ inner wall, ❑ antennae, + upper limiter.

2.5 Magnetic axis position

Initial examination of the magnetic axis position, as calculated by EFIT, and the neutron centroid showed a systematic discrepancy of about 10 cm. Reprocessing of the neutron data (see section 3.20) has resolved much of this discrepancy.

The two signals to compare are the EFIT magnetic axis (EFIT/RMAG) and the computed centroid of the neutron emissivity (KN3L/ROS) as shown in Fig 2.7, which shows the data before and after reprocessing.

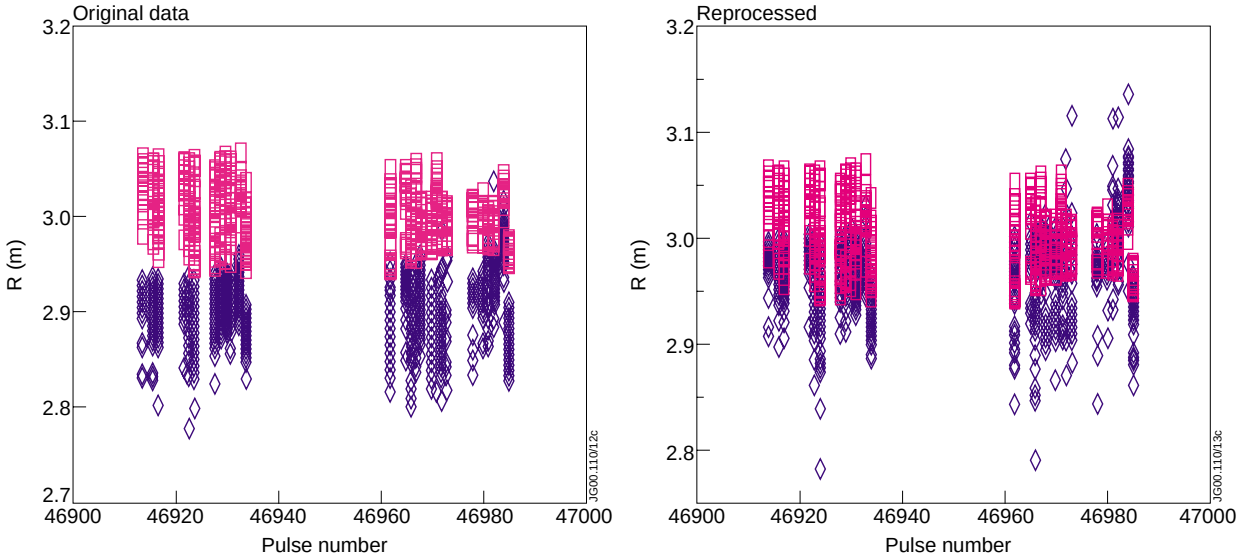

Fig 2.7: Comparison of the magnetic axis (EFIT) and the neutron centroid for ELMy H-mode discharges. The squares are the EFIT results and the Diamonds the neutron centroid

This improvement, due to reprocessing of the neutron data, is also evident from examining individual time histories of shots, as show in Figures 2.8 and 2.9.

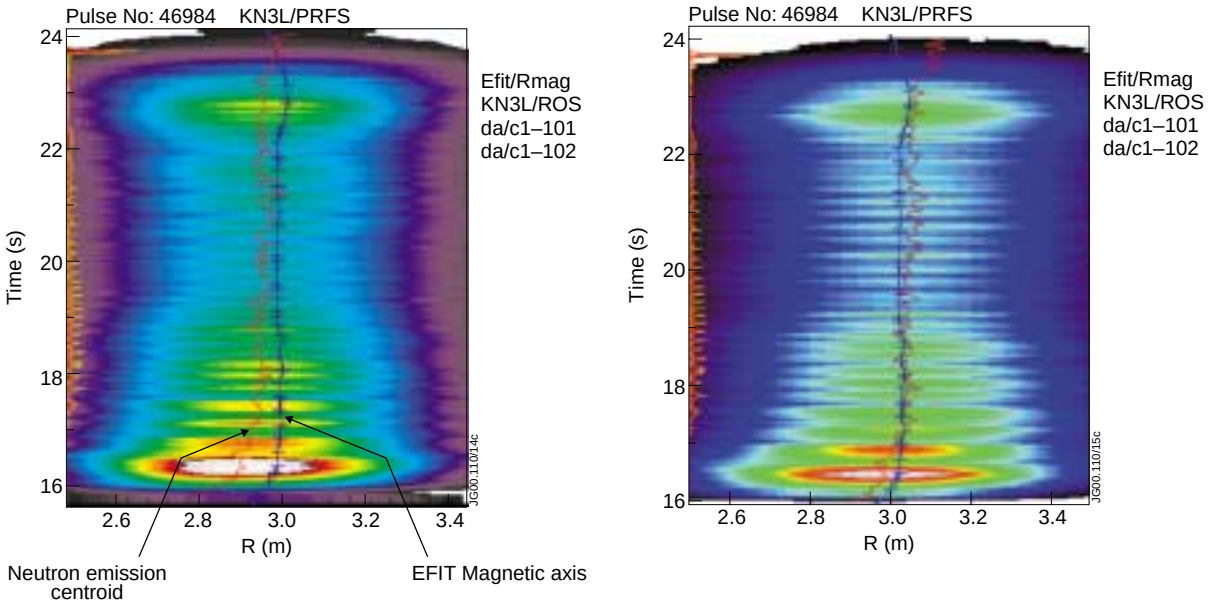

Fig 2.8 Typical ELMy H-mode pulse showing neutron emission contours with the neutron emission centroid inboard of the EFIT magnetic axis particularly during the high power heating phase (~16 to 17s) before the reprocessing and that this is corrected after reprocessing of the neutron data (left hand plot is before reprocessing and right hand plot is after).

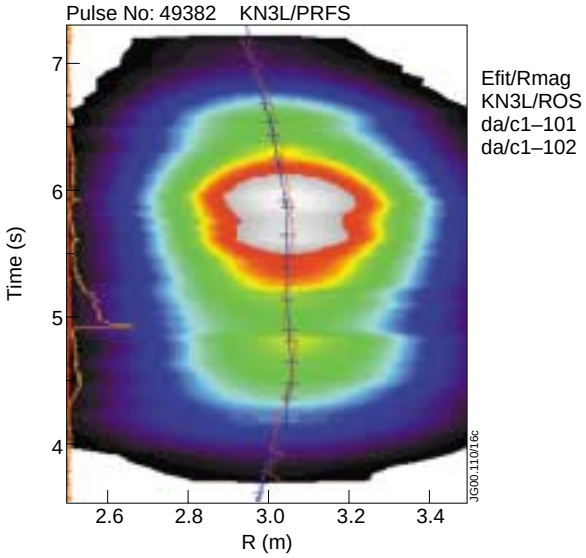

Fig 2.9 Optimised shear pulse showing good agreement of EFIT and neutron axis position after reprocessing. Note that SXR data of the instability just before 5s (see left hand trace which is the perturbed n=1 mode amplitude) indicates the magnetic axis is at 3.05m, which is also in good agreement.

2.6 TRANSP Comparisons

An overall check of data consistency can be made by using TRANSP - for the Autumn 1999 campaign data about 50 pulses have associated TRANSP runs. Generally with neutral beam heating TRANSP shows good data consistency. This is illustrated in Figs 2.10 and 2.11 for an ELMy H-mode and Optimised Shear discharge, respectively.

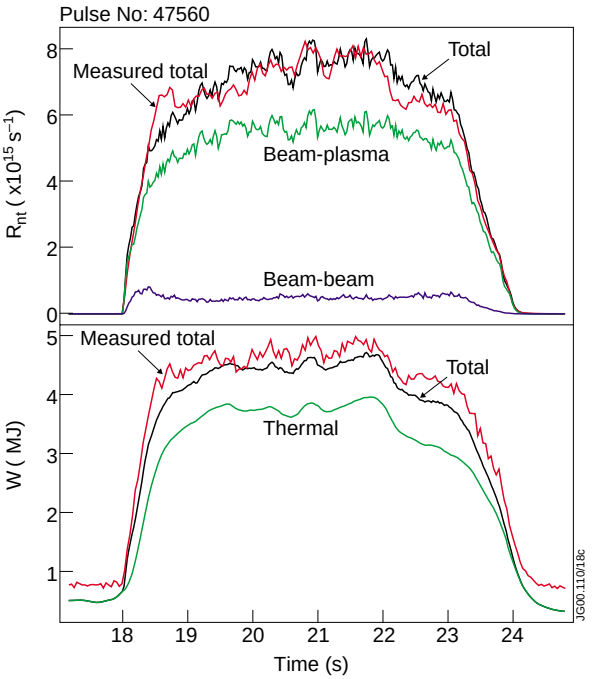

Fig 2.10 Comparison for ELMy H-mode pulse 47560, of TRANSP predictions for neutron rate (Rnt), and diamagnetic energy (W), with experimental measurements. Also shown are the various contributions to these quantities predicted by TRANSP.

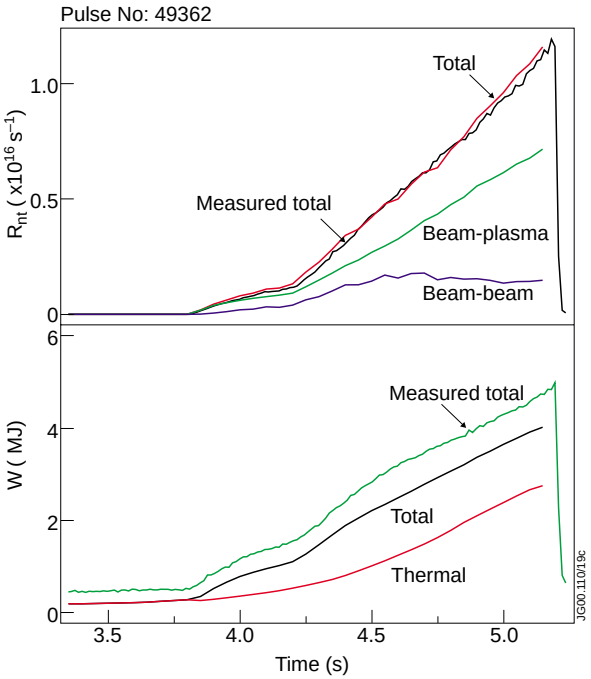

Fig 2.11 Comparison for Optimised Shear pulse 49362, of TRANSP predictions for neutron rate (Rnt), and diamagnetic energy (W), with experimental measurements. Also shown are the various contributions to these quantities predicted by TRANSP.

There is however a problem when there is strong ICRF heating, with TRANSP results. There are in principle two options to simulate the ICRF heating in TRANSP, a Monte-Carlo or a Fokker-Planck operator. The Monte-Carlo method is the more sophisticated but doesn't include heating of the fast deuterium beam tail by the ICRH (an important omission). The Fokker-Planck method, while less sophisticated, does include the tail heating. However, the Fokker-Planck method has yet to be implemented in the JET version of TRANSP (though it works at PPPL).

3. INDIVIDUAL DATA REPORTS

3.1 CHAIN2

Description:

The Second Processing Chain (CHAIN2) consists of a suite of ten programs which together provide a full local analysis of the bulk plasma physics within the JET Tokamak. Density, temperature, auxiliary power absorption, fast particles, radiation and transport coefficients are all calculated on equilibrium surfaces taken from EFIT.

Relevant DDAs:

C2DR ECM2 EQUI LID2 LOCO NBP2 NBP4 NBP8 NBPT NFT2 NION PION PRAD TION

Reprocessing:

CHAIN2 has run on a pulse per pulse basis on request. As part of the Data Validation Winding Up Contract a list of such pulses was provided and data produced. For each requested pulse the data from the KG1 Multichannel Far Infrared Interferometer has been manually corrected for fringe jumps to allow for processing by NFT2. As this needs to be done on all eight channels, to produce a reasonable profile reconstruction, this alone took considerable time.

As CHAIN2 depends on a lot of input PPFs, reprocessing is necessary whenever one of these PPFs has changed. CHAIN2 reruns on a regular basis over all pulses that need reprocessing. A list of Chain 2 pulses is given in Appendix A.

Comments on data:

None

RO

M Charlet

3.2 Charge Exchange

Description:

Charge eXchange Spectroscopy (CXS), radial profiles of ion temperature, toroidal rotation and light impurity densities (He, C, Ne, Ar). Consistency Checks (Line average Z_{eff}, neutron yield, W_{Dia})

Relevant DDAs:

CXS1 CXS2 CXS3 CXSM CXDM

Reprocessing:

As part of the data validation excercise, processing of basic data (T_i, ω_{tor}) was requested for about 150 discharges in the MkII-GB campaign. In addition, CHEAP analysis (Impurity concentrations, beam deposition calculations, consistency checks) was requested for about 70 discharges. These requests have been dealt with where possible (ie excluding discharges where the relevant Octant 8 Pinis were turned off and discharges where the CX hardware failed, see Appendix). To date (30/3/2000) some requests for data processing, notably in TF-P, have not yet been received, hence further processing is expected to occur before the end of the winding up contract.

In addition, we reprocessed (CHEAP analysis) 389 shots in the range 40297 to 43950 to incorporate the latest electron density and temperature data (from the KS3 PPF). Note that this reprocessing does not change the ion temperature and toroidal rotation results, but affects impurity densities and consistency checks.

Comments on data:

To assist operations in optimised shear discharges, an attempt has been made to provide basic analysis between shots for discharges without noble gas puffs for edge control. Other than that CXS data is produced only on request.

In the presence of the aforementioned noble gases, we do not have a reliable method to extract the required data from the CXS spectra on a routine basis. There are very few discharges with noble gas puffs where any CXS analysis has been performed. This lack of data is deliberate. For some discharges, an NBI notch method has been applied to help resolve the issues, details of this can be found in the relevant TF-B/C JET Report. We are presently working on new methods to analyse these data. When they will be available, we aim to reprocess all JET data with noble gas puffs. This is not likely to occur during the duration of the winding up contract.

In discharges with pellet injection, raw data quality is poor just after the pellet has been absorbed by the plasma, due to the enhanced beam attenuation in the plasma periphery. In addition, our beam deposition code has not yet been modified to make use of other density profiles but LIDAR. In between LIDAR time points, we interpolate the density, which is obviously wrong for pellet fuelled discharges. Therefore any results on impurity densities that are derived for these discharges should only be used at LIDAR times. We do not have the facility in our codes to suppress the output between LIDAR times.

RO:

K-D Zastrow

Appendix

The following discharges, although requested, cannot be analysed due to failure of the CXS hardware:

49139, 49167, 49180, 49583

3.3 CONL

Description:

The CONL code computes the connection lengths for a prescribed set of points determined by the divertor geometry. It uses as input equilibrium data to be obtained with EFIT and generates database relevant to plasma edge physics.

Relevant DDAs:

CONL

Reprocessing:

It has been requested for all MKIIGB pulses (# >/ 44414) in the steady state database.

Comments on data:

Data were produced for pulses in the range 31459 – 44379 for MKIIA configurations. (Last shot - 27.04.97). Then the code was removed from chain1 because it consumes too much CPU time.

RO:

Vladimir Drozdov

3.4 Divertor Pressure

Description:

In the past the pressure gauge diagnostic KY5D consisted of 15 ionisation gauges distributed in sets of five in octants 2, 4, and 8. The gauges are positioned between 2 and 5 cm below the divertor target surface with one gauge probing the inner corner position of the divertor (poloidal position 1) followed by two gauges at the private flux region (one closer to the inner strike zone, ie. poloidal position 2, and the other closer to the outer strike zone, ie. poloidal position 3), then a fourth gauge probing the outer corner of the divertor (poloidal position 4) and a fith gauge sitting in front of the cryo pump (poloidal position 5). A maximum of only five gauges can take data during a shot. The PGnn PFF with nm={21,22,23,24,25,41,42,43,44,45,81,82,83,84,85} with the first digit n of a two digit number nm gives the octant number in which the gauge is located and the second digit m gives the poloidal position of the gauge (see below for more details). Unfortunately only the PG24 gauge was left operational during the 1999 campaign (all other gauges being damaged over time).

Relevant DDAs:

PGnn

Reprocessing:

Standard PPFs produced: PGnn/{FLUX,PRES,DENS}

Comments on data:

Pressure gauges need calibrations with gas puff and toroidal field in a dry run. For each gauge that has been calibrated there is a standard calibration function that is a fit to many calibration data over a range of neutral particle pressures. The PPF’s normally use this calibration function and the associated uncertainty is between about +/- 50% and +/- 20% depending on the gauge. Data can be re-run with a more accurate calibration provided a calibration shot was done close to the discharge in question. For any detailed investigations turn to the DVRO. The gauges are sensitive in the equivalent pressure range of between 10**-5 mbar and some 10**-2 mbar. A change of the toroidal field can affect the reading of the gauges. This needs individual investigation. If the PPF show zeros only, this indicates that the gauge operated but was not

calibrated before; in this case relative information can be obtained from the JPF data. If the PPF show only noise the gauge did either not work or the pressure was too low. JPF data are only distinguished by the poloidal position number m. There are 3 different types of data:

(i) Filament current Y5-A1<CUR:00m , with m {1,2,3,4,5}. Typical values are between 1V and 1.5V if the gauge was on.

(ii) Electron emission current Y5-A2<EL:00m with m {1,2,3,4,5}. Typical values are above 2V if the gauge operated properly.

(iii) Ion current Y5-A2<EL:00m with m {1,2,3,4,5}. This signal is proportional to the neutral particle flux into the gauge. Values can reach 10 V (in Elmy periods).

RO

W Fundamenski

3.5 Divertor Thermocouples

Description:

Divertor tile thermocouples used for determination of deposited energy for whole pulse from cooling curves.

Relevant DDAs:

DVTC

Reprocessing:

Reprocessing has been carried out once for all pulses held in the steady state database. A further reprocessing is still required to account for changes in other DDAs which have influenced the results.

Comments on data:

This data only has a simple interpretation for steady state pulses where the equilibrium was not changed during the pulse. Data are available for all MkIIGB pulses but only processed for the steady state database.

RO

G Matthews

3.6 ECE

Description:

Multichannel Heterodyne Radiometer.

Relevant DDAs:

KK3 KK3P

Reprocessing:

A list of validated pulses is given in Appendix A.

Comments on data:

KK3 DDAs were produced routinely throughout 1999. KK3P DDAs are only produced interactively on request. It should be noted that KK3 measurements is not valid during LHCD heating.

RO

R Prentice

3.7 Edge Charge Exchange

Description:

Two arrays of near vertically viewing chords giving charge exchange measurements of carbon from the octant 4 beams. One set of chords gives high resolution (down to 2 cms) at the edge (outermost 30 cms), the other extends in to $\rho \approx 0.3$ at a resolution of 6 cms.

Relevant DDAs:

CXEP CXSE

Reprocessing:

No reprocessing has been done; data are routinely produced by the intershot analysis programs.

Comments on data:

In most cases edge Ti measurements are available. In some specific discharges the diagnostic was tuned to measure helium spectra, in these cases the routine analysis is inapplicable. In a few cases core measurements are available (although the routine analysis need modification for these cases).

RO

N Hawkes

3.8 EFIT

Description:

The EFIT – J (JET) code reconstructs MHD equilibrium of the JET plasmas using Grad-Shafranov equation constrained by external (magnetics) and optionally internal (polarimetry, MSE, etc.) measurements.

Relevant DDAs:

EFIT

Reprocessing:

About 50 shots (with fast magnetic data) from the last (autumn 1999) campaign were reprocessed for chain2.

11 shots (in the range 45903 – 47061) were reprocessed for chain1 with more homogeneous time vector distribution up to disruption.

Comments on data:

Data, based on external magnetic measurements, were produced routinely throughout 1999.

It can be observed (in particular for 97-99 campaigns) a moderate but a quite regular and persistent discrepancy in EFIT and MG3 plasma energy data, density data from KG1 and reconstructed from LIDAR-EFIT, etc. List of some “extreme” shots has been compiled and further investigation is required.

RO:

Vladimir Drozdov

3.9 ELMS

Description:

Calculates the ELM frequency from the vertical H-alpha signal.

Relevant DDAs:

ELMA ELMS

Reprocessing:

No reprocessing has been necessary.

Comments on data:

The data was produced routinely throughout 1999.

RO

M Johnson

3.10 GAS

Description:

Provides information on the volume of gases, rates of flow, gas species and electron counts of gases injected from the GIM’s into the vessel for a discharge.

Relevant DDAs:

GAS GASM

Reprocessing:

No reprocessing has been necessary as part of the winding up contract.

Comments on data:

Data was produced routinely throughout 1999.

RO

M Johnson

3.11 ICRH

Description:

ICRH system and codes.

Relevant DDAs:

ICRH RFA RFB RFC RFD CRH1

Reprocessing:

None required.

Comments on data:

ICRH data was produced routinely throughout 1999. CRH1 data, which describes the radial positions of the ion cyclotron resonances, is not available for pulses with poor coupling.

RO

D C McDonald

3.12 Bolometry

Description:

Total radiated power measured by the KB1, KB3 and KB4 bolometer systems.

Relevant DDAs:

BOLO BOL4 B3D4 B3E4

Reprocessing:

No reprocessing has taken place as the data is virtually independent of other diagnostics.

Comments on data:

The BOLO and BOL4 PPFs (based on KB1 data) were produced routinely throughout 1999. BOLO/TOPO has been calulated in a consistent way since 1994. The total radiated power (BOLO/TOPO) has recently been verified: in most plasmas it is between 0 and 10% too low; in some special cases BOLO/TOPO may underestimate the total radiated by more than 10% (see JET

Report JET-R(99)06 for details).

The B3D4 and B3E4 PPFs (based on KB3 and KB4 data) have not been produced routinely since the installation of the MkIIGB divertor, but have been produced on request with a limited number of channels for some discharges.

RO

C Ingesson

3.13 Calorimetry

Description:

KD1D divertor calorimetry data derived from the divertor thermocouples.

Relevant DDAs:

KD1D

Reprocessing:

No reprocessing necessary for the winding up contract.

Comments on data:

The data was produced routinely throughout 1999.

RO

M.Johnson

3.14 Interferometry

Description:

The diagnostic measures the line-integrated electron density along four vertical and four lateral chords (Channels 1 to 8) using far-infrared laser beams.

Relevant DDAs:

KG1V KG1L KG1B

Reprocessing:

Rather than reprocessing it is a peculiarity of FIR interferometry that the data have to be checked/ corrected for fringe jumps. This has been done for a large number of 1999 JET pulses on request - see list in Appendix A.

Comments on data:

Data was produced routinely throughout 1999.

It is strongly recommended that users of KG1V check the Status Flag of each channel they are going to use. A Status Flag equal to zero means that the data is unchecked!

Unchecked data may be used with caution (no guaranty!) if (i) there is no jump of the density at exactly 55 seconds and (ii) the pulse has not disrupted at its end. The 55 second check arises from the fact that fringes are corrected from the beginning of the pulse until 55 seconds and backwards from the end of the pulse until 55 seconds.

RO

K Guenther

3.15 Polarimetry

Description:

The diagnostic measures the Faraday rotation angle, which represents the line integral of electron density times projected component of the poloidal magnetic field, along four vertical and four lateral chords (Channels 1 to 8) using far-infrared laser beams.

Relevant DDAs:

KG4

Reprocessing:

Based on a new approach to calibrating and evaluating the measurements, all relevant data of the 1999 experimental campaigns have been reprocessed:

JET Pulses 46912 – 48382 and 48842 – 49802.

Comments on data:

Data was produced routinely throughout 1999.

Don't use data of pulses<46912. Note that during the first campaign (46912 – 48382) only the vertical channels 1 - 4 were working.

Status Flags are important: 1 - 3 refers to the degree of utilization of the available dynamic range while "0" indicates that there is at least one time value with an either saturated or too low signal level, which both results in a set value of an exact floating point zero.

RO

K Guenther

3.16 Langmuir Probes

Description:

Langmuir probes are mounted in the divertor target at a number of poloidal positions to measure the ion flux and other plasma parameters. Limiter and RF probe arrays are also active. Locations - Target: oct. 2 (Pop up) and oct. 5 (fixed), limiter inner wall guard oct. 1C, 3C, 5C, 7C poloidal limiter oct. 4B, 8B, RF antenna oct.6 along top protection tile. Fast collection using the CATS system (max. freq. 1 MHz) is available on a limited number of channels. The measurements are

reconstructed into spatial profiles of the parallel and surface ion flux in the form of a 3D PPF. In addition, the peak and integrated fluxes to the inner and outer divertor are calculated. The position of the peak ion flux may be used to identify the divertor strike point positions and provide an independent cross-check with results from the EFIT and XLOC code calculations

Relevant DDAs:

DOD KY4D

Reprocessing:

The electron temperature, density and surface power may be derived from the Langmuir probes, either in single or triple mode, using an interpretation program KY4DP in the IBM user space JETRDM, which produces private PPFs. (triple probes allow good time resolution in measurements of Te). Processing was carried out by the DVRO upon request, with dozens of shots from the 1999 data processed in this way. This data was used subsequently for onion-skin modelling (OSM2 code) of the scrape-off layer which allowed extraction of cross-field transport coefficients and impurity transport simulation (DIVIMP code).

Comments on data:

Langmuir probe data was produced routinely throughout 1999.

The accuracy of the Jsat and Te data is estimated at ~ 30% above 3 eV (the lower limit on Te measurement). Data is only available for probes that were activated; only probes which were active at the last calibration pulse (calibration shots were performed roughly every 1000 shots) were activated during normal JET discharges. Typically, fatigue in probe wiring is the cause of open-circuit probes. Data is not available outside of the specified time window, and below a specified cutoff. This explains the discontinuities in the data observed for probes in the outer SOL or in the private flux region. Sharp spikes in the data appear due to either ELMs or electrical arcs. For lower temperatures, ratio of hydrogen spectroscopic line (Hgamma/Halpha) should be consulted. Near the end of the 1999 campaign a calibration shot with triple probes was performed. This allowed for comparison of triple and single probes, showing good agreement in both Jsat and Te. Due to the geometry of the divertor, the major radius coordinate in the JSAT and JSUR DTypes below 2.411m and above 2.889m is artificial and corresponds to the distance along the vertical plate. In this case the signals for the position of the maximum ion flux centroid (RSIL, RSOL, ZSIL and ZSOL) should be used with caution. In the event that a probe has failed, the JSAT signal for that location will be written to the PPF with a value of -1 and may therefore be excluded by setting appropriate limits within the plotting program. Upon request it is possible to reprocess the PPF to interpolate the profile across the failed probe and recalculate the integrals. The ion flux is derived directly from the measurements at large negative bias rather than a full exponential fit to the I-V characteristic and may therefore be prone to underestimate the ion flux when the electron temperature exceeds 50eV. Field angles at the divertor target are derived from the XLOC code in order to calculate the projected area of the probe tips. In the event that this

information is not available the PPF will be assigned a status flag of 3 and certain DTypes (e.g. ANG) will be omitted.

RO

W Fundamenski

3.17 LHCD

Description:

LHCD system.

Relevant DDAs:

LHCD

Reprocessing:

None required.

Comments on data:

LHCD data was produced routinely throughout 1999.

RO

D C McDonald

3.18 LIDAR – Main LIDAR System

Description:

Measures electron temperature and density profiles on inclined (3^0) ~ horizontal diameter by time of flight Thomson back-scattering using a short (300ps) laser pulse.

Relevant DDAs:

LIDR LIDX

Reprocessing:

Regular comparisons of LIDR/TE and ECM1/PRFL Te data are run throughout the campaign to check that there is no divergence from normal agreement levels. No reprocessing of LIDAR data required for this cause in this campaign.

Regular comparisons of LIDX/LIDn and KG1V/LIDn data are also carried out throughout the campaign to check on the density calibration of LIDAR with respect to the Interferometer. This requires occasional correction of small amounts of PPF data.

Occasionally the spectral channel has too large a signal (background plasma light) or too small a time mark (used for automatic searching and setting relative timing of spectral channels in the analysis). This usually affects on or two time slices in one or two pulses in a series. The faulty time slices are located and a new PPF created if necessary.

Comments on data:

Te and ne profile data was produced routinely throughout 1999 for virtually all JET plasma pulses. However, due to a hardware failure corrected on September 28th 1999, no data from the first 18 physics discharges was produced.

RO

Chris Gowers

3.19 Magnetics

Description:

MAGN, MAGO	Currents and Fields, Timebase
MAGT	Fast sampled data near disruptions
MAGD	Backup to MAGN, not used
XLOC	Magnetic boundary, plasma position
MG2, MG3, MG4	Plasma position, Magnetic Boundary from FAST job
WIR	Lower X point position
DIA	Diamagnetic Flux loop
KIN	Total Energy measurement (depends on ECE
LAO	Plasma shape

Reprocessing:

None requested

Comments on data:

The Magnetic diagnostic systems have functioned without reported problems throughout the period under review.

The poloidal field coils were corrected for toroidal pickup by TF only shots 47163, 47598, 49040 (09-Feb, 09-Mar, 19-Oct-1999)

RO

J Conboy

3.20 Neutrons

Description:

The DDA TIN is derived from the set of calibrated fission chambers (KN1), plus some basic plasma information.

The DDAs DTN3 and KN3x are both derived from the neutron profile monitor (KN3). DTN3 is obtained from summing appropriately weighted data-channels and is highly robust. It gives the d-t neutron emission, which is be due to triton burnup plus any tritium content. KN3x is based on least-squares fitting and gives a detailed presentation of d-d or d-t data, as appropriate for the discharge.

Relevant DDAs:

TIN DTN3 KN3x

Reprocessing:

The KN31 analyses (d-t plasmas) are generally very good, but the KN3L analyses (d-d plasmas) could be improved. An upgraded analysis routine, which detects any spurious channels, has been found to give considerably improved results for d-d plasmas. A mass reprocessing of data from the Gas Box is in progress to correct the KN3L PPFs.

Comments on data:

Data for both diagnostics were produced on a routine basis throughout 1999.

RO

O N Jarvis

3.21 Pedestal

Description:

Pedestal data is produced by taking the marked position of the H-mode edge pedestal, from KK3P/RPED, and then interpolating density, temperature and fast particle profile data at this position.

Relevant DDAs:

PED

Reprocessing:

Reprocessing takes place weekly, to keep the data up to date with reprocessing done on the density, temperature and fast particle data. Further, when extra pulses have been marked (by KK3P) they are processed for PED.

Comments on data:

PENCIL artificially sets the edge value of the fast particles energy to zero, hence NBP2/ AENG(x=20) is usually a better measure of the pedestal mean fast particle energy than PED/ AEPP.

RO

D C McDonald

3.22 Penning Gauge

Description:

KT5P represents the two penning gauges which measure the sub-divertor neutral (molecular) pressure. PT5P contains the corresponding penning gauge spectroscopy with light collected from the penning gauge and fed into quartz optic fibres, which relay the light to the diagnostic hall. There the light from the fibres is analysed with a high-resolution visible spectrometer that uses a CCD camera as detector. PT5P PPF is derived from one track of the CCD camera.

Relevant DDAs:

KT5P PT5P

Reprocessing:

A multi-gaussian fit, with many constraints is used to fit the spectral data. The constrained parameters are: a) the warm D-,T- and H-alpha components all have the same ion temperature, b) all cold D-,T- and H- components have the same ion temperature, c) all hydrogen isotope components are shifted relative to their equivalent D-alpha counterparts by a given constant (the isotope shift).

Comments on data:

KT5P & PT5P data was produced routinely throughout 1999. Fits to the data are usually quite good, though at low count rates the errors on HTOT and TTOT, etc., may be as large as the signal itself. The accuracy of any particular fit may be judged by comparing the fitted spectrum with the raw data (nodes FIT and RAW), for the same time slice. The code for remembering the DDA Nodes is; H or D or T for hydrogen or deuterium or tritium, C or W for cold or warm component, and I for Intensity, P for Position and W for Line-Width. On occasions, the PC controlling the CCD camera loses contact with the PC server on DataNet. This results in no JPF, or PPF, until the fault condition is noticed, and the PC reconnected to the server.

RO

W Fundamenski

3.23 Pressure Gauges

Description:

Data from KY5 “penning gauges”.

Relevant DDAs:

PRES

Reprocessing:

No reprocessing required.

Comments on data:

The data was produced routinely throughout 1999.

RO

M Johnson

3.24 Scaling Laws

Description:

The PPF SCAL is produced using input data from MG3 and other PPFs processed by program TAUE. The diamagnetic energy and total input power are read from MG3/WPD and MG3/YTO respectively. A Gaussian smoothing is applied to each (FWHM 235ms) before calculating the confinement time, TAU. Various scaling law predictions of the confinement time, are evaluated using additional data from KC1D, LIDAR, and EFIT. There are also calculations of some general parameters of interest, such as the total radiated power fraction (using data from bolometers).

Relevant DDAs:

SCAL

Reprocessing:

The SCAL PPF is produced automatically after each pulse.

Comments on data:

SCAL PFF was produced routinely throughout 1999. SCAL assumes a pure deuterium plasma (M=2). The typical uncertainty for the confinement scaling predictions is expected to be in the range 10% to 20%, without considering the isotope dependence. The list of all scaling laws may be found in the JET data handbook. Note that some scaling laws predict the total confinement time, and others predict the thermal confinement time (i.e. without fast ions). The parameter TN93 is the ratio between the measured total confinement time, and the prediction of thermal confinement time using the ITER ’93 ELM-free H-mode scaling law. Comparison with this law is encouraged by those who study confinement scaling at JET, but it should be remembered that fast ions can cause this to be an over-estimate of confinement enhancement.

RO

W Fundamenski

3.25 Vessel Gauges

Description:

Vessel displacements and forces are calculated from displacement and strain gauge transducers.

Relevant DDAs:

VDIS VFOR

Reprocessing:

No reprocessing has been performed as part of the winding up contract.

Comments on data:

The data was produced routinely throughout 1999.

RO

M Johnson

3.26 Visible Spectroscopy

Description:

The KS3 diagnostic ('D-alpha and visible spectroscopy') monitors the visible radiation (plasma bremsstrahlung and spectral line emission) emitted by the plasma. Telescopes collect the plasma light and fused silica fibre-optic cables are used to transfer it to the Diagnostic Hall where it is analysed.

The KL2 diagnostic ('Flux cameras') consists of CCD cameras, located at the top of an Upper Main Vertical Port, with a direct view of the JET divertor. Interference filters are used to transmit only a single spectral line to each camera.

Relevant DDAs:

From KL2: KL2A KL2B KL2C

From KS3: KS3A KS3B KS3D KS3H KS3I KS3O S3A2 S3AD S3D2 EDG6 ZEFF

Reprocessing:

During consistency tests of our Calibration Lamps it was discovered that some calibration drifts (upto 20%) had occurred. To resolve which Lamp was in fact the accurate one, one was returned to the manufacturer for recalibration. On its return we were able to calculate corrections for the other Lamps.

During March 1999, a rare intermittent fault with the KS3 LeCroy HV Power Supply, which supplies HV to the photomultiplier (PM) tubes, became more common, and started to impinge on JET operation. The LeCroy HV Crate was changed, with only a temporary improvement, but when the HV pods were changed the fault was cleared.

The new HV Power Supply provided slightly different voltages to the PM tubes, giving a noticeably different PM tube gain on

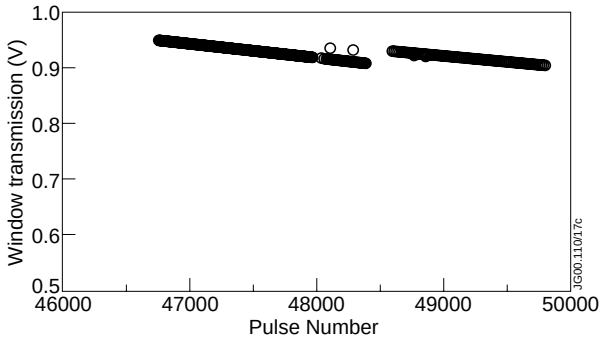

Window Transmission used in PPF (Black line) and measured transmission (circles). As part of the data reprocessing this modest discrepancy in transmission was corrected.

several channels. Corrections had been calculated and implemented at the time, but PM tube data for a few pulses (during the troubleshooting) were uncorrected.

Consequently, reprocessing of EDG6, which contains the PM tube data, was carried out for the affected pulses.

Comments on data:

JPF and PPF data was produced routinely throughout 1999. Some reprocessing has been necessary, as detailed above.

Since the absolute transmission of the KS3 windows was not measured during the shutdown at the end of plasma operation in 1999, the KS3 PPF's all contain a 'best guess' of the transmission of the relevant window. This fact, together with the added uncertainties caused by the Calibration Lamp drifts, and the HV power supply problem, reinforce the warning that systematic errors (e.g. on Z-effective) between different campaigns could easily be 20-30%.

RO

M Stamp

3.27 VUV Spectroscopy

Description:

KT2 VUV survey spectrometer and KT4 VUV/XUV spectrometer

Relevant DDAs:

T2I0 (KT2), T4I1, T4I2 (KT4), UVIN (both instruments)

Reprocessing:

The UVIN PPFs are calibrated versions of the T2I0, T4I1 and T4I2 PPFs. The calibration process for KT2 and KT4 is ongoing and depends on various factors such as the KS3 calibration, which is not finalised at present. Some UVIN generation should take place before the end of the winding up period.

Comments on data:

Spectral line intensity time histories were routinely produced by both instruments for all major impurities (both intrinsic and extrinsic) during 1999.

RO

I Coffey

3.28 Pellet Centrifuge

Description:

Inboard and Outboard pellets injected into plasma.

Relevant DDAs:

CE

Reprocessing:

Carried out when required during 1999. Two pulses (48829 and 48853) reprocessed in 2000.

Comments on data:

A Bickley was responsible for the pellet data produced after the inboard pellet launcher was introduced in September 1999 (pulse 48643 onwards). PPFs created before this date have not been checked.

The following eight PPFs do not contain outboard pellet data due to a hardware fault: 49045 to 48, 49075 to 76, 49082, 49462.

RO

A Bickley

3.29 Neutral Beam Injection

Description:

Neutral beam power injected to plasma from octant 4 (80kV) and octant 8 (140kV).

Relevant DDAs:

NBI, NBI4, NBI8

Reprocessing:

Carried out when required during 1999. No new reprocessing necessary.

Comments on data:

Data was produced routinely throughout 1999.

RO

A Bickley

3.30 XLOC

Description:

The XLOC code reconstructs JET plasma boundary or separatrix in x-point configurations. The interpretive procedure is based on magnetic measurements and local expansion technique. A real time version of XLOC is also used at JET for plasma shape and position control.

Relevant DDAs:

XLOC

Reprocessing:

No requests.

Comments on data:

Data were produced routinely throughout 1999.

RO:

Vladimir Drozdov

3.31 X-Ray Crystal Spectroscopy

Description:

High resolution X-ray crystal spectrometer, observing resonance line of He-like Nickel

Relevant DDAs:

XCS

Reprocessing:

No reprocessing was done as part of this contract

Comments on data:

Data was produced routinely throughout 1999. The overall quality of the signal is poor for two reasons. Firstly, the amount of Nickel in JET has been decreasing since the cladding of the inner wall. Secondly, the present detector is 14 years old and has lost sensitivity. A new detector is presently being commissioned and should become available later this year.

RO

K-D Zastrow

4. SUMMARY

The work undertaken on data validation under the JET Joint Undertaking winding-up agreement falls into two broad categories:-

- Checks of the individual data consistency by the ROs for each diagnostic (as summarised in Section 3)
- Request from the Task Forces to validate the data from specified diagnostics for a specified list of pulses (see Appendix A for details)

As a result of the data consistency checks several large scale reprocessing exercises have been undertaken. This major reprocessing involves the mass reprocessing of shots due to a new calibration measurement or an improvement in a data processing code. The major reprocessing undertaken as part of the winding-up agreement has been for the recalibration of the visible spectroscopy data (see section 2.4), for the KG4 polarimetry data (see section 3.14), the improved

code for the KN3 data (see sections 2.5 and 3.20), the EFIT data and the XLOC data. The EFIT data was reprocessed because of a coding problem resulting in the diamagnetic energy being incorrectly calculated (EFIT/WDIA) and, similarly, the XLOC data was reprocessed because a coding problem led to the angle of the strike points on the divertor tiles (XLOC/ASTK) being incorrectly calculated. While the visible spectroscopy data was reprocessed to correct for an incorrectly calibrated calibration lamp and polarimetry data was reprocessed to exploit an improved calibration procedure.

The two Task Forces produced prioritised lists of about 500 pulses each, for validation of specified diagnostics. This validation is now over 90% complete with the entire exercise expected to be completed by mid May (validated pulses are listed in Appendix A). The largest of these validation exercises proved to be that for the interferometer, where in particular the pellet pulses were particularly difficult and time consuming to validate. The ECE (KK3) validation has also proved to be a lengthy exercise.

So in summary, the validation and required reprocessing of the 1999 Gas Box is largely complete and the data is being actively used by the Task Forces for descriptive and further data analysis.

APPENDIX A: LISTS OF VALIDATED SHOTS

The lists presented here are correct at the 17 May 2000. The most update list are accessible from the JET web address /data.jet.uk/dcc.

A.1 KK3 ECE data

KK3 data is generally reliable, but the automated calibration procedure can be wrong. The following shots were validated

47952	47955	47956	47958	48651	48652	48653	48654	48655	48656
48658	48659	48662	48663	48675	48677	48678	48701	48704	48705
48706	48707	48970	48971	48974	48994	49006	49017	49126	49128
49129	49130	49131	49133	49134	49136	49137	49138	49139	49140
49144	49145	49152	49153	49154	49156	49157	49159	49160	49161
49164	49168	49197	49263	49264	49265	49270	49272	49275	49309
49310	49314	49315	49320	49323	49362	49381	49382	49384	49410
49443	49547	49557	49566	49572	49579	49586	49591	49592	49596
49615	49616	49617	49618	49619	49620	49621	49622	49623	49630
49647	49651	49654	49655	49665	49680	49682	49683	49705	49726
49727	49728	49729	49730	49731	49732	49739	49755	49758	49759
49760	49761	49762	49789	49791	49793	49794	49796		

The following requested shots could not produce good data, mainly due to the fields and currents of the particular discharges.

49547	49557	49566	49572	49573	49579	49581
49582	49586	49591	49592	49596	49596	49726
49727	49728	49729	49730	49731	49732	49739
49566	49572	49573	49579	49581	49582	49586
49591	49592	49596	49596	49726	49727	49728
49729	49730	49732	49739	49547	49557	49731

A.2 KG1V interferometry data

KG1V data requires a manual fringe correcting procedure. Due to the time required to correct all 8 channels, only the central chord is corrected when fast profile data is not required. The following shots have all channels validated

49794	49793	49788	49786	49762	49761	49739	49737	49736	49735
49734	49733	49732	49731	49730	49729	49728	49727	49726	49723
49720	49712	49709	49708	49707	49706	49705	49704	49703	49702
49701	49700	49699	49698	49697	49696	49694	49693	49692	49691
49690	49689	49688	49687	49685	49683	49682	49680	49677	49675
49673	49672	49670	49655	49654	49652	49651	49647	49630	49596
49592	49591	49583	49582	49581	49579	49573	49557	49556	49555
49554	49553	49551	49550	49547	49520	49514	49512	49447	49443
49441	49437	49436	49421	49418	49384	49382	49369	49366	49362
49323	49320	49318	49315	49314	49313	49310	49309	49300	49275
49273	49272	49271	49270	49269	49266	49265	49264	49263	49262
49221	49220	49214	49209	49208	49186	49185	49182	49181	49180
49173	49172	49170	49169	49168	49167	49166	49165	49164	49161
49160	49159	49157	49156	49154	49153	49152	49151	49149	49147
49146	49145	49144	49140	49139	49138	49137	49136	49134	49133
49131	49130	49129	49128	49126	49023	49022	49021	49020	49018
49017	49015	49014	49012	49008	48678	48381	48380	48362	48361
48360	48359	48347	48346	48342	48339	48338	48337	48336	48333
48325	48304	48301	48300	48298	48297	48295	48293	48277	48276
48272	48271	48270	48269	48265	48264	48262	48261	48260	47958
47956	47955	47952	47852	47851	47849	47843	47828	47816	47805

47804	47803	47797	47796	47793	47767	47763	47762	47761	47758
47757	47670	47669	47668	47649	47647	47646	47620	47615	47614
47585	47584	47583	47578	47577	47576	47575	47574	47572	47571
47570	47569	47568	47567	47565	47564	47563	47562	47561	47560
47559	47558	47556	47555	47554	47553	47551	47550	47549	47548
47546	47545	47543	47542	47541	47540	47538	47536	47530	47524
47523	47522	47521	47520	47519	47517	47516	47514	47513	47512
47509	47508	47507	47505	47501	47500	47499	47496	47495	47494
47486	47485	47484	47483	47482	47481	47480	47479	47478	47476
47424	47420	47414	47413	47316	47314	47313	47310	47309	47308
47307	47306	47304	47303	47302	47301	47300	47299	47297	47293
47287	47286	47284	47283	47281	47280	47279	47278	47277	47276
47275	47274	47170	47115	47110	47103	47101	47066	47039	47023
47010	46998	46985	46984	46982	46981	46980	46978	46973	46972
46971	46970	46967	46966	46965	46962	46933	46931	46930	46929
46923	46922	46917	46916	46914	46836	46834	46833	46829	46828
46826	46825	46824	46822	46821	46819	46818	46816	46815	46814
46813	46807	46806	46805	46804	46800	46799	46798	46794	46792
46695	46464	45406							

The following shots were validated for the central chord (LID3) only

49760	49759	49758	49757	49756	49755	49724	49695	49676	49668
49666	49549	49548	49519	49516	49511	49510	49504	49503	49501
49498	49478	49477	49476	49475	49474	49473	49472	49471	49470
49456	49358	49357	49355	49352	49339	49338	49336	49335	49334
49333	49332	49331	49321	49319	49317	49316	49312	49311	49308
49307	49306	49268	49267	49252	49251	49250	49249	49248	49247
49244	49239	49082	49080	49079	49078	49068	49065	49056	49054
48994	48365	47813	47623	47305					

Finally, the following shots could not provide useful data

49566	No JPFs
49304	No JPFs
49302	No JPFs
49301	No JPFs
49064	JPFs for horizontal lines of sight (5,6,7,8) only
48358	JPFs for vertical lines of sight (1, 3, 4) only
47811	JPFs for vertical lines of sight (1,3,4) only

A.3 CHARGE EXCHANGE

Charge exchange data needs individual manual reprocessing to produce accurate ion temperature profiles. Further data is produced by the running of the modelling code CHEAP. The following shots have been validated for ion temperatures and CHEAP.

46593	46600	47516	47517	47519	47520	47521	47522	47523	47524
47527	47528	47529	47530	47531	48970	48971	49138	49146	49164
49197	49263	49264	49265	49270	49272	49275	49309	49310	49314
49315	49320	49323	49418	49421	49436	49437	49441	49654	49685
49689	49696	49697	49698	49699	49700	49701	49702	49703	49704
49705	49706	49707	49708	49709	49726	49727	49728	49729	49730
49731	49732	49733	49734	49735	49736	49737	49739	49794	

The following shots have been validated for ion temperatures only

49126	49128	49129	49130	49131	49133	49134	49136	49137	49138
49139	49140	49144	49145	49146	49147	49149	49151	49152	49153
49154	49156	49157	49159	49160	49161	49164	49165	49166	49167
49168	49169	49170	49172	49173	49180	49181	49182	49185	49186
49204	49205	49206	49207	49208	49209	49362	49374	49375	49376
49377	49378	49379	49380	49381	49382	49383	49384	49443	49547
49557	49566	49572	49573	49579	49581	49582	49583	49586	49591
49592	49596	49629	49630	49633	49636	49637	49641	49643	49644
49645	49647	49651	49652	49666	49668	49670	49672	49673	49675
49676	49677	49680	49682	49683	49755	49756	49757	49758	49759
49760	49761	49762	49791	49793	49794	49796			

Shots with noble gases (notably Argon) are discussed in the TF B/C JET Report.

A.4 TRANSP

TRANSP runs provide a valuable means for data validation. TRANSP runs have been performed on the following shots by UKAEA workers. Further runs have also been made at Princeton.

48970	48971	49197	49362
49443	49654	49655	49793
47952	47955		

A.5 LIDAR

The LIDAR diagnostic is very reliable and data is generally assumed to be good. However, LIDAR data validation was requested and carried out for the following shots.

49129	49130	49131	49133	49134	49136	49137	49138	49139	49145
49146	49147	49149	49151	49160	49161	49164	49165	49166	49167
49168	49547	49557	49566	49572	49579	49586	49596		

A.6 MSE

MSE data has been validated on the following shots

49382	49384	49630	49647	49651
49680	49682	49683		

A.7 CHAIN2

The running of the CHAIN2 codes provides valuable information on data validation. The following shots have been validated by CHAIN2.

46800	46805	46806	46813	46814	46815	46816	46818	46819	46821
46822	46824	46825	46826	46828	46829	46833	46834	46836	46914
46916	46917	46922	46923	46929	46930	46931	46933	46962	46965
46966	46967	46970	46971	46972	46973	46978	46980	46981	46982
46984	46985	46998	47023	47039	47066	47103	47213	47274	47275
47276	47277	47278	47279	47280	47281	47283	47284	47286	47287
47293	47297	47299	47300	47301	47302	47303	47304	47306	47307
47308	47309	47310	47313	47314	47316	47352	47410	47413	47424
47425	47476	47478	47479	47480	47481	47482	47483	47484	47485
47505	47509	47513	47516	47517	47519	47520	47521	47522	47523
47524	47530	47536	47538	47540	47541	47542	47543	47545	47546
47548	47549	47550	47551	47553	47554	47555	47556	47558	47559

47560	47561	47562	47563	47564	47565	47567	47568	47569	47570
47571	47572	47574	47575	47576	47577	47578	47583	47584	47585
47614	47615	47620	47667	47668	47669	47670	47711	47716	47717
47742	47743	47744	47749	47757	47758	47762	47763	47767	47793
47796	47797	47803	47804	47805	47816	47818	47821	47843	47849
47851	47852	48202	48203	48204	48260	48261	48262	48264	48265
48269	48270	48271	48272	48276	48277	48293	48295	48297	48298
48300	48301	48304	48325	48333	48336	48337	48338	48339	48342
48357	48358	48359	48360	48361	48362	48867	48868	48870	48872
48873	48970	48971	49008	49012	49014	49015	49017	49018	49020
49021	49022	49023	49029	49030	49044	49054	49056	49065	49078
49080	49081	49082	49126	49128	49129	49130	49131	49133	49134
49136	49137	49138	49139	49140	49144	49145	49146	49147	49149
49151	49152	49153	49154	49156	49157	49159	49160	49161	49164
49165	49166	49167	49168	49169	49170	49172	49173	49180	49181
49182	49185	49186	49197	49208	49209	49214	49220	49221	49225
49238	49243	49244	49246	49247	49248	49249	49250	49251	49252
49263	49264	49265	49270	49272	49275	49291	49293	49297	49309
49310	49314	49315	49320	49323	49362	49366	49369	49382	49384
49443	49447	49454	49456	49503	49504	49547	49550	49554	49555
49566	49572	49573	49579	49581	49582	49583	49586	49591	49592
49596	49630	49647	49651	49654	49655	49680	49682	49683	49689
49696	49697	49698	49699	49700	49701	49702	49703	49704	49705
49706	49707	49708	49709	49712	49720	49723	49726	49727	49728
49729	49730	49731	49732	49733	49734	49735	49736	49739	49761
49762	49793								